Analysis of Thermal and Mechanical Behavior of Copper Molds during Continuous Casting of Steel Slabs

B. G. Thomas, G. Li, A. Moitra, and D. Habing

Mechanical & Industrial Engineering Dept.,
University of Illinois, Urbana, IL 61801
(217)-333-6919

ABSTRACT

Three-dimensional finite-element thermal-stress models are applied to predict temperature, distortion and residual stress in a continuous casting mold for steel slabs. The model predictions of temperature, distortion during operation, and residual distorted mold shape match plant observations. During operation, the copper faces bend towards the steel, with a maximum outward distortion on the order of 1mm, found just above the center of the wide faces. Distortion during operation increases with increasing mold temperature, increasing strand width, and decreasing water jacket rigidity. Mold clamping forces, bolt prestress, friction, and ferrostatic pressure have little effect on this behavior. Constraint generated by the temperature gradients and the sides of the bolt holes in the steel water jackets generate stresses and creep in the copper hot face during operation. This leads to permanent distortion and residual stress after cooling to ambient. Residual stress and distortion increase with repeated thermal cycling over a campaign, higher temperatures, smaller water-jacket bolt holes, non-uniform water slot depth, and higher clamping forces. Increased residual distortion requires increased remachining, which reduces mold life. Increased residual stress increases the probability of a catastrophic crack failure.

1. INTRODUCTION

During continuous casting, the copper mold plates control the shape and initial solidification of the steel product, where quality is either created or lost. Maintaining a reliable, crack-free mold within close dimensional tolerances is also crucial to safety and productivity. The costs associated with mold maintenance are a significant fraction of the operating costs of a caster. Thus, it is important to understand the thermal and mechanical behavior of the mold.

During operation, large temperature gradients develop across the copper plates, which causes them to warp. Although the amount of distortion is small, it is important because it changes the size of the gap between the shell and the mold, which controls heat transfer.

Distortion also affects how the different mold components contact together and wear. The plates also wear due to constant abrasion against the strand as it is withdrawn.

After cooling to ambient, the plasticity and creep that was generated during long hours of operation at high temperature causes residual stresses. The mold plates must withstand this stress reliably without cracking, because the consequences of water leaking through the mold would be catastrophic.

After many cycles of heating and cooling, permanent residual strain and distortion are generated in the copper plates. After a number of heats, constituting a "campaign", the plates must be remachined to remove the effects of both wear and distortion. The mold is discarded when the copper plates are reduced to less than a minimum allowable thickness, so the mold lifetime decreases with increased remachining.

This work was undertaken to provide insight into slab mold behavior using three-dimensional (3-D) finite-element models of heat transfer and stress. The results are compared with plant measurements and evaluated to offer suggestions regarding mold design and operation to improve mold life, safety, and steel quality.

2. PREVIOUS WORK

Several significant studies have applied mathematical models to understand the thermal and mechanical behavior of single-piece tube molds for casting steel billets [1-4]. This behavior was found to be very important to heat transfer, dimensional accuracy, strand quality, and life of the billet mold tubes. Samarasekera et al. [4] developed an alternating direction implicit finite difference heat conduction model, combined with a finite element stress model to predict the temperature, distortion, and stress fields in a billet mold wall under different operating conditions. During operation, the mold wall distorted outward (away from the molten steel) according to the mold temperature. The maximum distortion of 0.1 to 0.3 mm was found 90 mm below the meniscus. Above the meniscus bulge, the mold wall assumed a negative taper of 1-2 %/m, while a positive taper of 0.4%/m was produced below [4]. Strains were greatest near the meniscus and varied with the meniscus level and the type of mold constraint. Increasing copper wall thickness or decreasing water velocity increased the peak temperature, distortion, and stress in the mold.

This predicted behavior was confirmed by experiments which monitored temperature and mold movement in an operating billet caster [4]. Mold distortion, especially the negative taper near the meniscus, was held responsible for transverse depressions and cracks. Other problems including billet rhomboidity and longitudinal corner cracks were attributed to asymmetric mold distortion, which was caused by asymmetric boiling heat transfer and made worse when the top of the mold was constrained on only two sides, rather than all four. Mold distortion, as influenced by mold geometry,

constraint, and thermal loading is clearly a critical concern in avoiding quality problems in billet casting.

Relatively less effort has been invested to understand the mechanical behavior of slab molds. Hashimoto et al. [5] modeled temperature, distortion, and thermal stress in a fully-constrained slab mold plate including creep, and predicted a permanent 0.2 to 0.3 mm contraction of the wide face after repeated thermal cycling, depending on the copper properties. Thinning the mold plate was found to reduce the temperature, distortion, and stress. They also observed that the presence of horizontal water slots had little effect on mold plate deformation so should be omitted from the design. The corners of vertical water slots with square roots were found to act as sites for stress concentration [5]. More residual deformation was predicted when bolt-hole clearance was small.

Tada et al. [6] studied the factors affecting the performance and service life of continuous casting slab molds. Care in choosing mold clamping forces and plating the mold with Ni-Fe or Ni-W-Fe plating was reported to triple the mold life. Hot face temperature was lowered using deeper water slots. They also emphasized the importance of designing and maintaining the cooling water delivery system to ensure high, uniform velocity in each cooling slot. This improves uniformity of heat transfer, with resulting improvements in mold life and reduction in sticking corner breakouts.

Thomas [7] applied an elastic finite element model to predict temperature and distortion of a slab mold during operation. The wide faces were predicted to bend inward (toward the steel) with a maximum distortion on the order of 1 mm on the wide face centerline between the meniscus and mold mid-height.

Ozgu [8] instrumented a slab mold to measure a wide range of operating parameters, including mold wall temperature and deformation. The measured distortion behavior was consistent with the predictions of Thomas.

O'Conner and Dantzig [9] applied an elastic-plastic-creep finite element model to predict temperature, thermal distortion, stress, and hot face cracks in a funnel-shaped mold for casting thin slabs. Fatigue cracks were attributed to over-constraint of the copper plates, although the steel water jacket was not modeled.

Salkiewicz and coworkers [10] measured the effect of copper alloy properties on permanent distortion and wear of 25 mm thick copper mold plates in a cassette mold. Copper CCZ alloy plates revealed a large width contraction of the plates, that was 3X greater across the top than the bottom. The plates also "sagged, creating a convex-downward shape across the top and bottom of the plates. High wear was measured very near the mold bottom. Low-conductivity, high creep-resistant alloys had little or no residual distortion, and less wear.

This previous work has shown that temperature and distortion of the mold is important to mold life and

steel quality. The present study aims to quantify slab mold temperature, distortion and stress during operation as a function of design and operating variables, using realistic finite element models, and to derive practical insights into mold behavior.

3. MOLD CONSTRUCTION

Thermal - mechanical behavior of the mold depends on its construction and constraint. The mold for slab casting includes four separate copper plates, as shown in Figure 1. As shown in the top view in Figure 2, the narrow faces can slide between the wide faces to vary both the width of the mold cavity and the taper, as desired. Narrow face position can be monitored and controlled accurately using inclinometers.
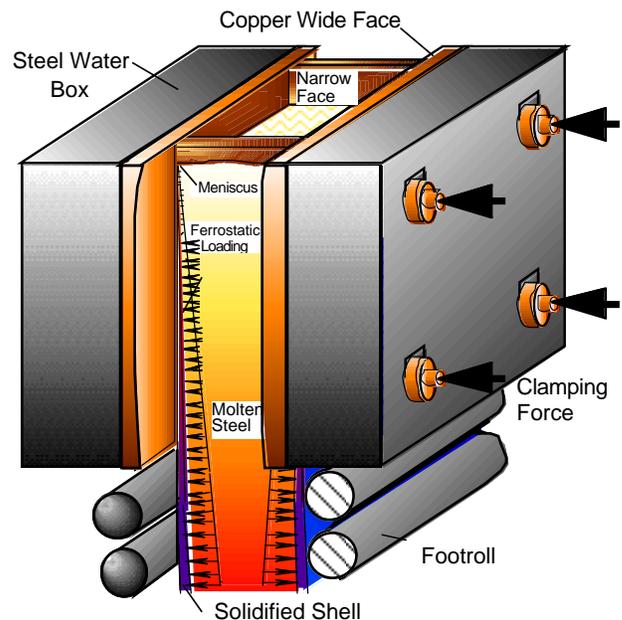

Figure 1 Cutaway of continuous casting mold showing loading on the wide face copper plates.
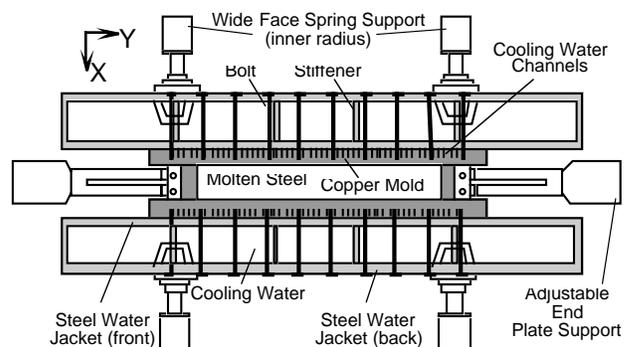

Figure 2 Schematic top view of mold

A close-up of a representative portion of the wide face top view is given in Figure 3. Long parallel vertical channels or "slots" for cooling water are machined into the back of each copper plate. Each plate is then bolted to

the steel box or "water jacket", which controls the distribution of cooling water into the bottom of the slots and collects the heated water which exits from the top of the slots. The bolts connect the copper plate with the back of the water jacket. They are relatively free to slide both axially and laterally through the unthreaded water jacket, because the bolt holes on the front plate are oversized. The bolts are spaced evenly every 4 - 6 slots, depending upon the design. Usually, the space between the two water slots that straddle a column of bolts must be greater than the space between the other slots, as shown in Figure 4.
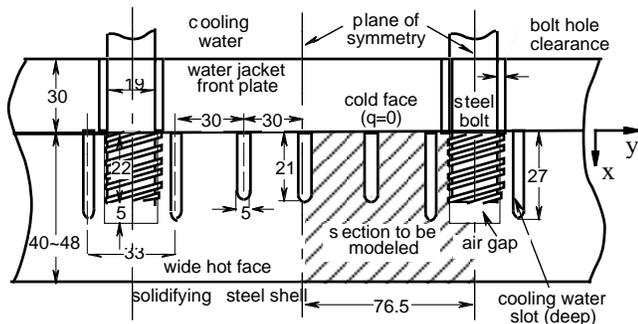

Figure 3 Close-up of representative horizontal section through wide face showing model domain and standard dimensions
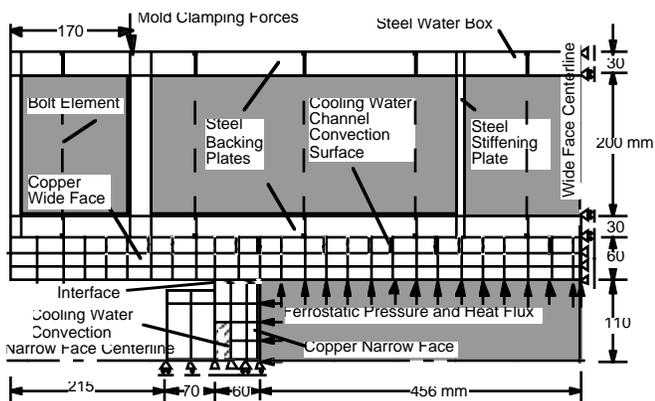

Figure 4 Top view of 3-D quarter mold model showing boundary conditions (Table I Conditions)

The steel water jacket also provides rigidity to partly restrain the bending of the copper plates due to the huge temperature gradients which are imposed during operation. The outer radius wide face water jacket (fixed side) is attached to a huge steel frame (not pictured) that surrounds the entire mold assembly. The inner wide face (loose side) is clamped through adjustable spring loading devices with sufficient force prevent the mold assembly from coming apart during operation.

In contrast to slab mold construction, a billet mold consists of a single piece of thin walled tube held within an outer box. Water flows through the space between them. A bloom mold that is machined from a solid copper block likely behaves in a similar manner to the billet mold and differently from the slab mold.

4. MODEL DESCRIPTION

Finite-element models were developed to calculate temperature, displacement, plastic deformation, creep strain, and stress in typical slab casting molds during steady operating conditions and after cooling to ambient. Model domains include typical two-dimensional (2-D) vertical and horizontal sections through the copper plates, a 3-D model of a representative vertical segment of the mold, and a complete 3-D model of one quarter section of the mold, including the water jackets and bolts. Standard conditions for the 3-D quarter mold are given in Table I, while standard conditions for the other models are given in Table II.

Table I. Standard Simulation Conditions I

Mold Geometry	
Slab width	914 mm
Slab thickness	220 mm
Mold height	700 mm
Cu plate thickness	60 mm
Water slot depth - shallow slots	25 mm
Water slot thickness	5 mm
Distance between most slots	35
Distance between slots across bolt	48
Bolt diameter	19 mm
Bolt length (water jacket thickness)	280 mm
Distance between bolts	114 mm
Copper properties	
Thermal conductivity	374 W m^{-1}K^{-1}
Elastic modulus	117 GPa
Poisson ratio	0.343
Thermal expansion coefficient, α	17.7 x10^{-6} K^{-1}
Density	8940 kg m^{-3}
Steel Properties	
Thermal conductivity	49 W m^{-1}K^{-1}
Elastic modulus	200 GPa
Poisson ratio	0.30
Thermal expansion coefficient	11.7 x10^{-6} K^{-1}
Density, ρ (for ferrostatic pressure)	7860 kg m^{-3}
Operating conditions	
Water slot heat transfer coef.	35 kW m^{-2}K^{-1}
Water temperature, T_w	15 ^{o}C
Ambient temperature	35 ^{o}C
Meniscus level (below mold top)	84 mm
Mold clamping forces	
top (.658 m from bottom)	8.9 kN each
bottom (.154 m from bottom)	22.2 kN each

Table II. Simulation Conditions II

Mold Geometry

Slab thickness	220 mm
Mold height	900 mm
Cu plate thickness - top & bottom	40.8 mm
- inner radius mid-mold	49.6 mm
Water slot depth - shallow slots	21 mm
- deep slots	27 mm
Water slot thickness	5 mm
End of slots (from mold top)	30 mm
Slot radius of curvature (y-z plane)	65 mm
Start slot curvature (from mold top)	81 mm
Distance between most slot centers	30 mm
Distance between slots across bolt	33 mm
Bolt diameter	19 mm
Distance between bolts	Fig. 5
Copper thermal conductivity (CCZ)	350 Wm^{-1}K^{-1}
Copper elastic modulus	130 GPa

Operating conditions

Water slot heat transfer coef.	35 kWm^{-2}K^{-1}
Water temperature	15 $^{\circ}$C
Ambient temperature	35 $^{\circ}$C
Meniscus level (below mold top)	130 mm

4.1 Heat Flow Model

Temperature during operation, T, is calculated by solving the steady heat conduction equation using linear-temperature finite elements.

$$\nabla \bullet k\nabla T = 0 \qquad (1)$$

where k is the thermal conductivity of the steel or copper. Heat was input to the exposed surfaces of copper elements on the mold hot faces as a function of distance both across and down the mold. Standard conditions, which are based on Savage and Pritchard for typical casting of low carbon steel at about 1 m/min [11], include heat flux functions below the meniscus,

$$q = 2.68 - 258\sqrt{0.616 - z}, \quad 0.0 < z < 0.616m \qquad (2)$$

where z is distance above mold exit, and above meniscus,

$$q = 2.68 + 31.9(0.616 - z), \quad 0.616 < z < 0.7m \quad (3)$$

This function includes a peak heat flux, q, of 2.68 MW/m^2 at the meniscus. To simulate the larger interfacial gaps near the corners, heat flux beneath the meniscus from the corner to 31 mm along the off-corner region of the wide face and narrow faces was decreased to 67% of standard wide face values. The standard water-slot heat transfer coefficient, h, of 35 kWm^{-2}K^{-1} is based on the experimental correlation of Sliecher and Rouse [12] assuming a water velocity of 8 m/s and no boiling.

The 3-D segment model domain, pictured in Figure 5, reproduces the complete geometric features of a typical repeating portion through the copper wide face using a refined mesh. This model imposes classic convection boundary conditions on all surface elements of the cooling water slots,

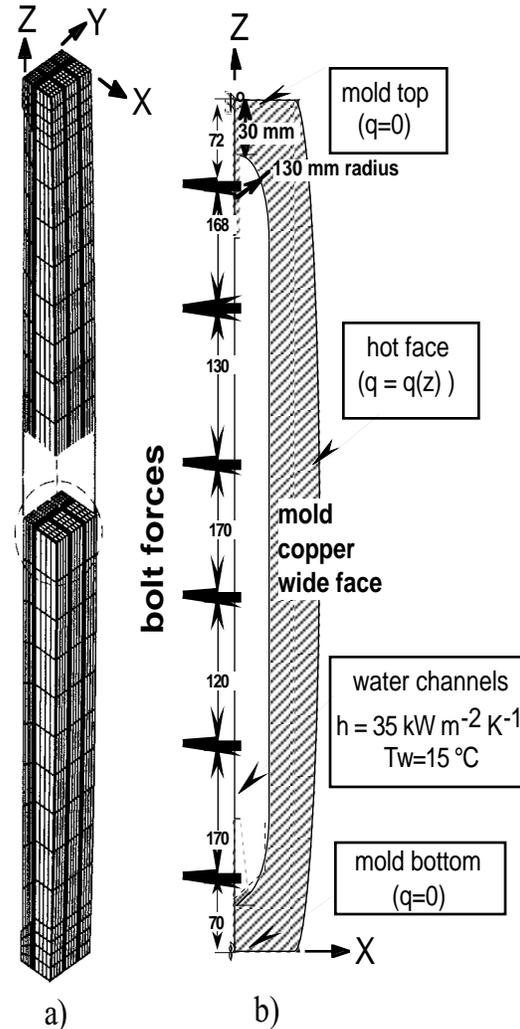$$q = h(T - T_w) \qquad (4)$$

Figure 5   3-D segment model domain showing:
a)   Finite element mesh
b)   End view of mold, showing geometry of water slot, bolt positions, and boundary conditions

The 3-D quarter-mold model represents each cooling water slot as a single convection boundary between two appropriate elements within the mold. This allowed a relatively coarse, carefully-designed mesh to extract the correct total amount of heat from approximately the right places in the mold. The accuracy of this approach was validated using the refined 3-D model of a representative slice. The quarter-mold model does not include geometric details such as mold curvature and the slot ends. Stress results for the coarse mesh are not as accurate as the other models, so the distorted shapes presented do not include creep. The 2-D model domains are shown in Figures 3 (transverse section) and 5b) (vertical section). Symmetry planes of all models are insulated (q=0).

4.2 Stress Model

Displacements, strains, and stresses are calculated by solving the standard equilibrium, constitutive, and strain-displacement equations using the finite element method [13]. The total strain, ε_{total}, is divided into components as follows:

$$\varepsilon_{total} = \varepsilon_{elastic} + \varepsilon_{thermal} + \varepsilon_{plastic} + \varepsilon_{creep} \qquad (5)$$

Elastic strain is directly proportional to stress according to the elastic modulus of each material, given in Table I. Thermal strain, $\alpha(T-T_0)$, is based on cycling between the ambient temperature, T_o, and the operating temperatures calculated by the heat flow model. This elastic-plastic-creep stress model assumed isotropic hardening with a temperature-dependent yield stress function, shown in Figure 6. The creep strain is determined incrementally in each time step by integrating a creep law for Cr-Zr copper, shown in Figure 7, based on data from Ratka et al. [14].
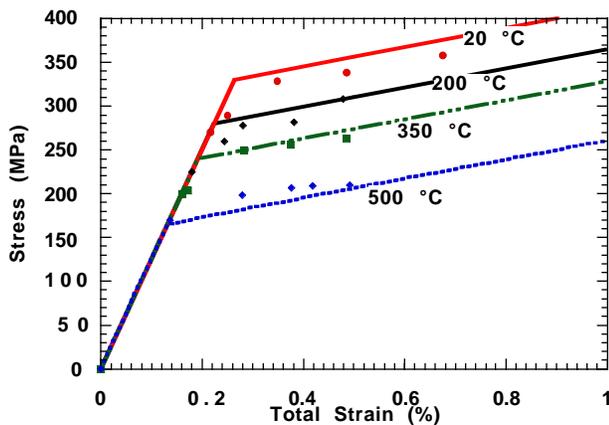

Figure 6   Stress strain curves for copper (Cr-Zr alloy) used in model (lines) compared with data [24] (points)
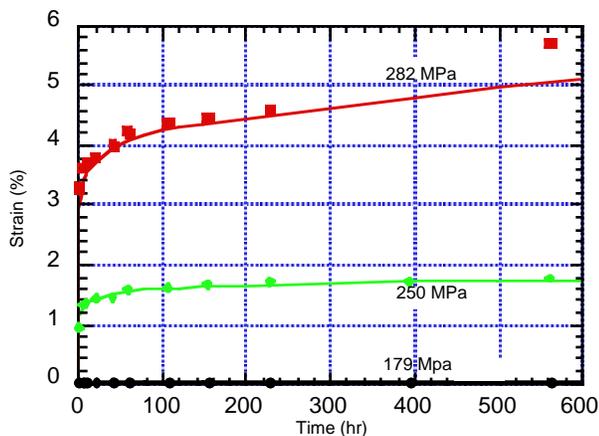

Figure 7 Creep curves for Cu-Cr-Zr alloy used in model compared with measurements [14]

For primary creep, t<100hr,

$$\dot{\varepsilon} = 2.48 x 10^{14} \exp\left(\frac{-197,000}{8.31\,T(K)}\right)\left[\sigma(ksi) - 23.\right]^{3}\left[t(s)\right]^{-0.92} (6)$$

For steady creep, t > 100 hr,

$$\dot{\varepsilon}(s^{-1}) = 1.54 x 10^{-10} \exp\left(\frac{-197,000}{8.31\,T(K)}\right)\left[\sigma(ksi)\right]^{14} \qquad (7)$$

The 3-D quarter-mold model includes separate domains for the mold coppers and water jackets which are coupled mathematically only at those points where they connect mechanically in the caster during operation. The cold side of the copper wide face is mathematically bolted to the back side of the water jacket at 30 locations using two-node bar elements. Since there are no threads in the water jacket itself, the bolt elements are constrained only to move vertically and horizontally with the water jacket back side. Bolts are pulled by the expanding copper plates during operation, which usually exceeds the applied pre-tension. A top-view of a typical mesh for this model is shown in Figure 4. Boundary conditions include ferrostatic pressure loads, ρg (0.7-z), over all hot-face surfaces and clamping forces on the exterior of the water jacket (Table I).

Elements along the top and bottom of the copper wide face are constrained from penetrating into the water jacket when they deform. The small region of contact between the edge of the narrow face and the wide face is modeled by coupling the x displacements of the contact points, which are found by trial and error. Finally, rigid body motion is prevented by constraining the symmetry planes from normal expansion and fixing a single point. This 3-D quarter-mold model neglects the spaces occupied by the cooling water slots, so overpredicts distortion and stress.

The 3-D segment model domain is pictured in Figure 5. To allow the sides of the segment to expand, while constraining them to remain straight, all normal (y-direction) displacements along one of the vertical (x-z) side planes were set to zero. In addition, a generalized plane strain condition was imposed on all elements on the other vertical (x-z) side:

$$\varepsilon_y = a_1 + a_2\,x + a_3\,z \qquad (8)$$

where two additional degrees of freedom in the model domain, constants a_1 and a_3, are calculated during the simulation. Rotation about the z axis was prevented by setting a_2 to zero. This is a reasonable approximation for the condition of a segment of a copper plate near the wide-face centerline. The other unconstrained sides, representing the hot and cold faces (y-z side planes) and the top and bottom (x-y planes) were left stress-free. Finally, the bolt forces were strategically adjusted to values of 1.2, 22.7, 10, -0.3, -2.6, and 15.5 kN, in order to account for the effect of the water jacket, which was not part of the model domain.

The 2-D transverse-section stress model used the same boundary conditions on ε_y as the 3-D segment model to allow uniform expansion of the edges representing the x-z side planes. In addition, the entire

domain was constrained to remain planar by imposing a constant strain condition on the undiscretized z direction.

$$\varepsilon_z = a_1 \qquad\qquad (9)$$

This was accomplished using special elements (GPE4) which have an additional translation degree of freedom (calculated to find a_1) and two additional rotational degrees of freedom (set to zero).

4.3 Solution Details

The finite element equations were solved and results visualized using the commercial stress-analysis package, ABAQUS 5.5 [15] on an IBM RS6000 workstation. The heat transfer and mechanical calculations are run sequentially, using the same mesh of 8-node, 2x2x2 Gaussian quadrature elements for each 3-D analysis. The 3800 node 3-D quarter-mold model requires 6 minutes execution time for the heat transfer calculation and 20 minutes for an elastic stress simulation. An elastic-plastic-creep simulation with the 10,200 node 3-D segment model required about 20 hours. The creep simulation required about 200 time steps to simulate 100 hours of operation, increasing from 1×10^{-8} s initially to a final time step size of over 3×10^{5} s. The 2-D models contained about 1800 nodes and executed quickly.

5. TYPICAL RESULTS

The typical temperature and distorted shape of the quarter mold model during operation is shown in Figures 8-10 for standard conditions (Table I).
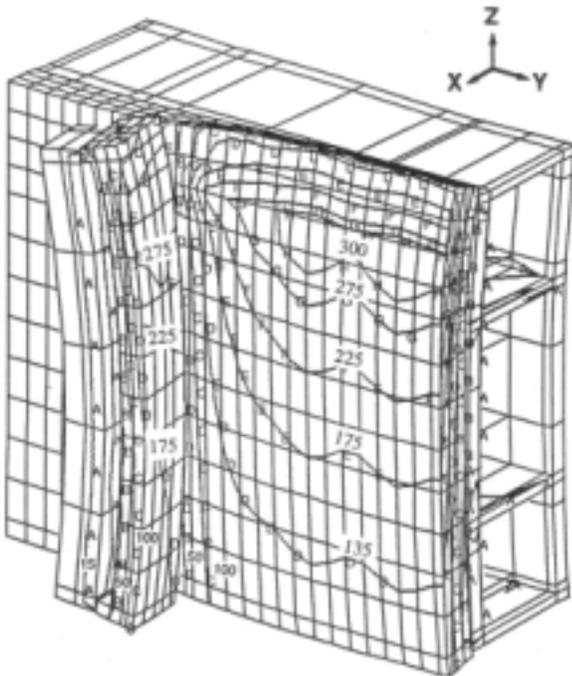

Figure 8 Temperature contours on distorted mold shape during operation (quarter mold model)
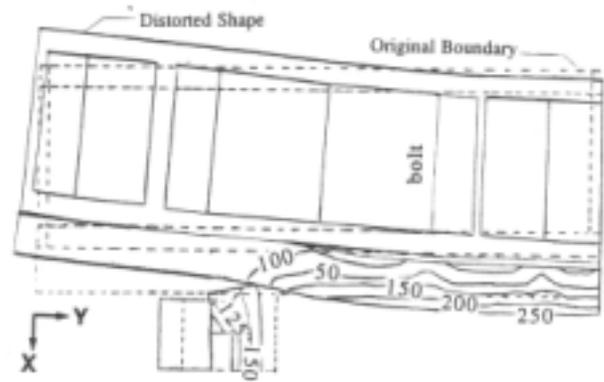

Figure 9 Top view of quarter mold (at z=0.5m) showing temperature contours and distorted shape during operation
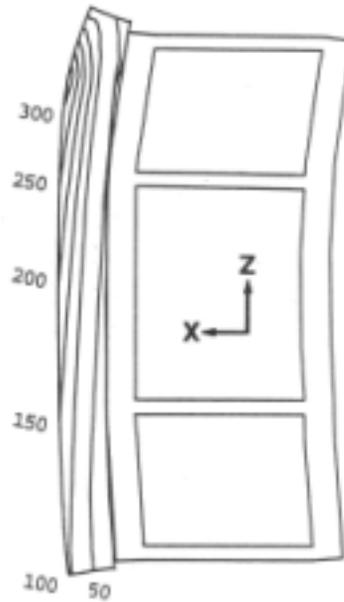

Figure 10   End view of distorted mold (wide face centerline) showing gap between copper and water jacket

Figure 8 shows the mesh, temperature contours on the hot face, and the distorted shape of the mold, exaggerated 50-fold. The maximum temperature is found on the hot face surface about 15 mm below the meniscus. The maximum surface temperature varies from 327°C (between bolts) to about 360°C, (opposite from the bolt, where water slot spacing is much larger). The cooling water channels keep the cold face and entire water jackets well below 100°C. A linear temperature gradient is established in the copper plates between the hot face and roots of the cooling water slots.

The results shown in Figures 8-10 provide insight into mechanical behavior of the mold during operation. The copper hot face expands in proportion to its temperature increase, but is restrained by the cold copper beneath it. Consequently, the copper plates bend outward toward the molten steel. The peak distortion, about 0.7 mm for standard conditions (Table I), occurs

below the meniscus along the center of the wide face. This distortion pulls on the restraining bolts, which also bends the exposed back side of the water jacket. The water jacket opposes this thermal distortion, depending on its rigidity.

The highest temperature in the mold is found along the corner of the narrow face near the meniscus, when narrow face and wide face heat flux are the same. This is because the narrow face cooling water slots in the simulated mold did not extend close enough to the edge of the narrow face. Heat flow from the narrow face to the wide face is insignificant due to the poor contact. The consequence of a high narrow face edge temperature is severe because this region of the mold also experiences the greatest stress concentration. The thin line of contact between the narrow face and the wide face must transmit all of the mold clamping forces.

Because the narrow face is connected to the wide face only through clamping pressure, the wide face is free to rotate around the expanded narrow face, contacting only along a small portion of the front vertical edge of the narrow face. As the wide face rotates outward, far away from its original position, a gap of several mm opens at the back of the narrow face. This ability to rotate is responsible for the difference in thermal distortion between slab molds and single-piece molds.

The bending copper plates stretch the bolts and pull away from the front of the water jacket during operation. Without bolt prestress, a thin gap forms, as shown in both Figures 9 and 10. The gap in a 40 mm thick mold varies from just over 0.2 mm where distortion is greatest (between the meniscus and midway down the mold) to about 0.1 mm in the lower half of the mold. Bolt prestress can prevent this gap between the copper plate and the water jacket and the detrimental penetration of water and scale formation which may accompany it.

Typical results for the evolution of mechanical behavior of the copper mold plates during the first casting heating and cooling cycle are presented in Figures 11-14, based on Table II conditions. Thermal distortion predicted by the 3-D segment model is given in Figure 11. Figures 12 and 13 show the corresponding stress - total strain histories in the width direction of points on the hot face and cold face of the copper plates at the meniscus, using the 2-D model. Figure 14 shows stress contours in a 2-D transverse section at two critical instants during the cycle.

After filling the mold with steel to start casting, thermal expansion of the heated copper hot face at the meniscus is resisted by the cold side of the copper. Slight additional constraint is also provided by the colder copper above and below the meniscus region, and possibly the bolts against the bolt holes in the front of the water jacket. Together, these partially restrain the hot face expansion. This generates compressive stress during operation (although the total strain is positive, as shown in Figure 12). This stress then induces "inelastic", or permanent strain from plastic flow and creep, which

partially relieves the stress. The result is a slight decrease in mold distortion with time during operation, as shown in Figure 11. Creep is highly temperature dependent, increasing ten-fold with only a 30°C increase in mold temperature from 265 to 295°C, based on Eq. 7. Creep also depends greatly on stress, so decreases with time as the stress is relieved. Thus, the difference in shape and stress between 8 and 100 hours of operation at elevated temperature is very small.
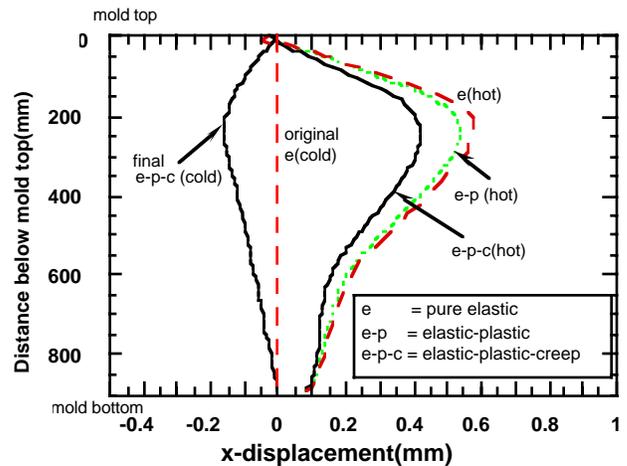

Figure 11 Predicted evolution of thermal distortion on vertical section through mold at bolt (3-D section model) for first heating / cooling cycle (100 hours creep)
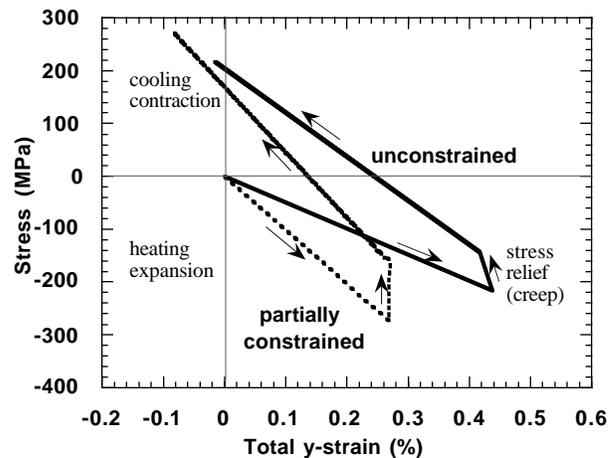

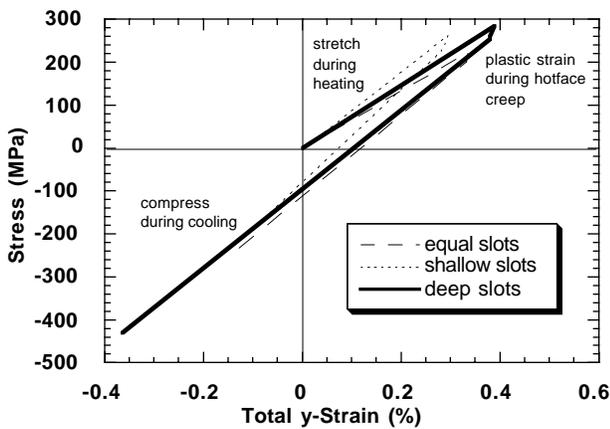Figure 12 Y-Stress-total strain history at copper hot face

Figure 13 Y-Stress-total strain history at water slot roots (first heating-cooling cycle)

After the mold cools to ambient temperature, stress would return to zero if there were no stress relaxation due to inelastic strain while hot. However, the accumulation of inelastic strain is responsible for permanent mold distortion. Residual distortion is clearly evident in this alloy. Thermal contraction during cooling reverses the hot face stresses to tension, causing the shape of the plate to reverse and bend away from the steel backing plate at the mold edges. The resulting "springback" illustrated in Figure 11 can be observed when the plates are unbolted from the water jacket. The residual tension also causes the plate width to shrink (bow tie effect), as the total strain becomes negative (Figure 12).

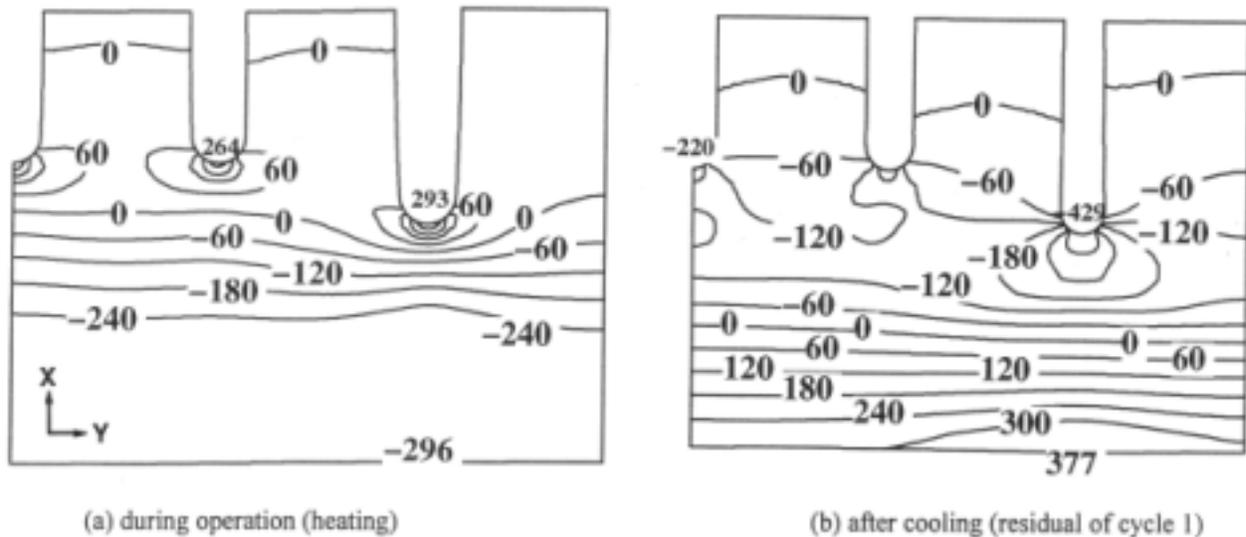(a) during operation (heating) (b) after cooling (residual of cycle 1)

Figure 14 Y-Stress Evolution in 2-D distorted mold section with deep slots (MPa) (partially constrained) (magnified 20X)

During elevated temperature operation, the general expansion of the hot face generates tensile stress and strain in the cold face (Figure 13). This strain concentrates at the roots of the water slots, (Figure 14) making them yield in tension. Then, during cooling, the high tensile stress at the surface forces the cold face into compression. In extreme cases, strain concentrated at the roots of the water slots may cause further yielding in compression.

Over a long time with high mold constraint, this alternating inelastic strain accumulation due to thermal cycling might lead to fatigue cracks through the copper faces, propagating from the roots of the cooling water slots. Residual distortion and stress are greatest near the meniscus region, where the highest temperatures and corresponding highest creep rates are generated.

6. MODEL VALIDATION

6.1 Temperature

To verify these model predictions, comparisons with experimental measurements were sought. The predicted mold temperature profiles are based on measured heat flux profiles, such as shown in Figure 16. The results are generally typical of reported temperature profiles [5,16-18] and the validity of this approach has been established in previous work by others including Brimacombe and coworkers.
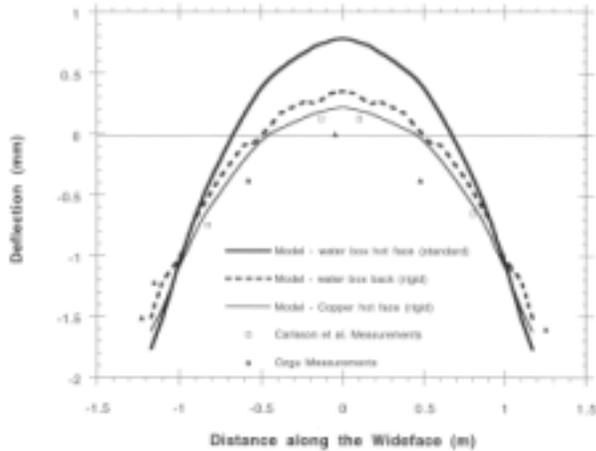
Figure 15 Comparison of calculated and measured [8] [19] back plate distortion during operation.
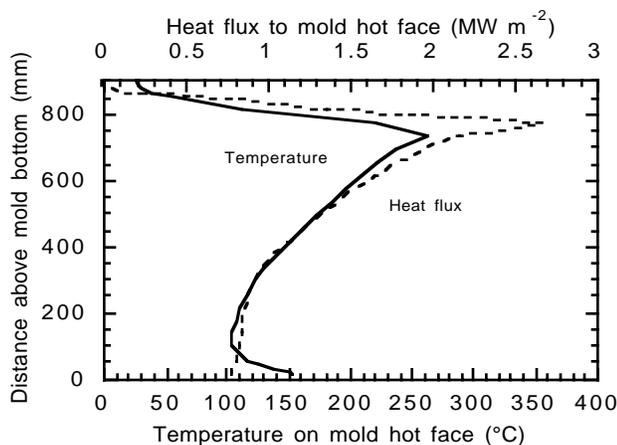

Figure 16 Heat flux and calculated temperature down hot surface of copper wide face inside radius (Table II conditions)

Within about 50 mm of mold exit, however, the 3-D segment model predicts that temperature increases by about 50°C (Figure 16).   This occurs despite a continuously decreasing heat flux profile.   This effect, which has been neglected in previous heat flow models, is due to the end of the water slot 30 mm above mold exit (Figure 5). This is the same location where Salkiewicz et. al. [10] measured a 2-7 fold increase in wear. This indirectly validates this novel prediction of the model, as copper is much more prone to creep at higher temperatures and has reduced strength, making it wear faster.

6.2 Distortion During Operation

Only a few slab mold distortion measurements have been performed during operation. Carlsson et. al. [19] and Ozgu [8] both used displacement transducers to measure the distortion at several different locations across the cold back face of the water jacket. Carlsson measured a 1680 x 220 x 785 mm mold for 8-30 minutes of casting and found displacements to stabilize about 5 minutes after the start of casting. Other conditions were not reported. Ozgu measured a 2350 x 260 x 700mm mold with 55mm

thick standard copper plates and 25mm deep water slots, casting a 1933mm wide slab at Bethlehem Steel.   The heat-flux profiles, extracted from thermocouple measurements, are similar to those from Eqs. 2 and 3, but are about 1.3X higher (rather than lower) on the narrow face.

A simulation was conducted to match the conditions of Ozgu. Unreported conditions were taken from Table I except that the water jacket was assumed to be more rigid, with a thickness of 320 mm and 40 mm thick steel plates. The predicted maximum wide and narrow face temperatures are 302 and 370°C, which are within the range of measured values. The predicted shape of the back of the water jacket midway up the mold is compared with measurements on the loose (inner radius) side in Figure 8. Displacements in this figure are all relative to the original position of the fixed side. Because the centerline through the narrow face is the fixed reference point in the model, the calculated distortion of the fixed side relative to the narrow face centerline (-0.60 mm) was added to each calculated x-displacement in constructing this figure.   Calculations are reflected to show the entire mold width.

The calculated distortions agree with the experiments both qualitatively and quantitatively: the mold shape becomes convex as it distorts inward towards the liquid steel at the center of the wide face and outward at the extremities. The model slightly overpredicts this distortion, which was expected due to 1) treating the water slots as solid in the 3-D quarter mold stress model and 2) the Bethlehem Steel mold actually having a stiffer 340 mm water jacket made with 45 mm thick plates).

The water jacket conforms closely to the copper when the bolts are prestressed, so the shape of the hot face is very near to that of the water jacket back plate in Figure 15.   The maximum displacement, found between the midpoint and meniscus on the wide face, is about 0.8 mm (relative to the narrow face centerline). These results are similar to those in Figure 8 because the increased distortion due to the greater width of the strand is compensated by the decrease in distortion from increased water box rigidity.

6.3 Residual Distortion

The 3-D segment model predictions of residual shape qualitatively agree with observations.   The predicted residual shape in Figure 13 is consistent with the observed lifting up, or "springback" of the copper plate edges after unbolting it from the water jacket. The predicted springback is 0.2 mm over the mold length, (Figure 11) but measurements for Table I. conditions could not be found.

Evaluation of the residual strain predictions (Figure 12) reveals that the predicted permanent mold width contraction, or "bow tie" varies from -0.02% (unconstrained) to -0.08% (partially constrained) for Table II conditions.   This is comparable with measurements after the first campaign (-1.02mm or -0.06%) made by Salkiewicz [10] on a cassette-type slab mold with 25mm

thick copper plates and a maximum slab width of 1680 mm. The maximum width contraction is predicted at the top of the mold, which is consistent with measurements. Permanent residual strain after the first heating cycle is predicted to be much larger than after subsequent cycles, due to the plastic strain and creep in the first cycle which relaxes the subsequent stress levels. However, measurements after subsequent campaigns reveal a roughly constant decrease in width for each campaign, leading to a total width contraction of 8.4 mm (0.5%) after 8 campaigns. Strains of this magnitude were not predicted by the model in subsequent cycles. This suggests that differences in the design and operation of the cassette mold may contribute to the phenomena.

Measurements also reveal a "sag" of 4-5 mm [10] at the center of the plates. This is likely caused in part by rotation about the plate normal (x axis) due to the greater width contraction of the top of the plates. This is complicated by creep phenomena in the vertical direction. Gravity forces appear to be negligible, as shown in Appendix III. Unfortunately, a complete quarter-mold model with a mesh refined like the 3-D segment model would be required to test this hypothesis.

7. PARAMETRIC STUDIES

Having validated the model and understood the basic thermal and mechanical behavior of the mold, the effect of different design and operating variables was investigated.

7.1 Effect of Water Slot Spacing and Depth

Copper temperature depends mainly on the heat flux transferred across the interfacial gap from the molten steel, and on the minimum distance between the copper hot face and the root of the nearest water slot. Thus, water slot geometry has a critical effect on temperature and accompanying thermal distortion and stress in the mold. Locations in the mold where cooling slots are farther from the surface thus incur higher hot face temperatures.

Care is especially needed in designing the cooling water slots on the narrow face, to ensure that they extend close enough to the narrow face edge. Cooling this edge is critical to strengthen this region of high stress concentration. Similar observations [20] have led to improved water slot design.
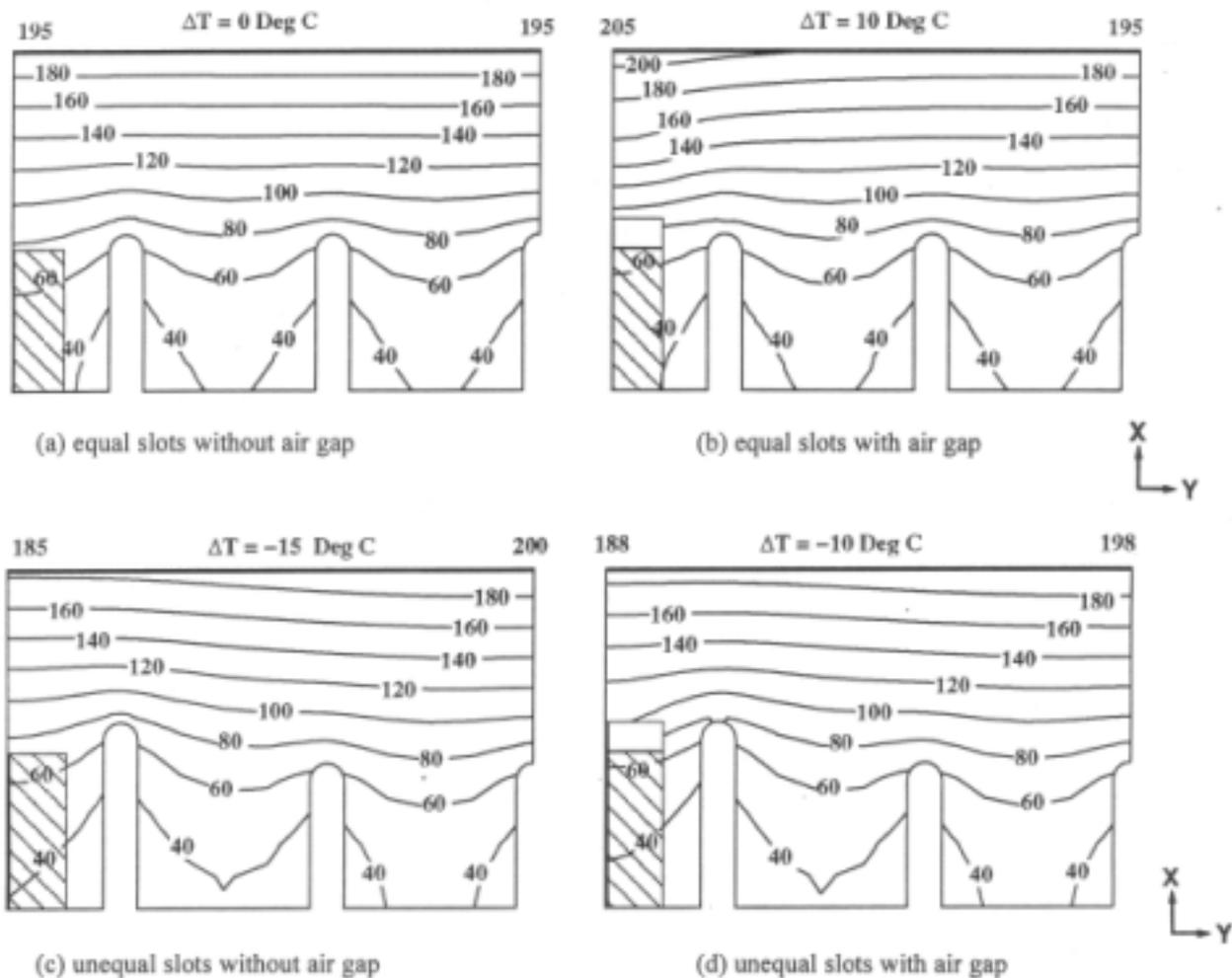

Figure 17   Effect of air gap beneath bolt hole and deep slot on temperature distribution (3-D section model)

Water slots often have a larger spacing across bolt locations. This leads to local temperature increases on the hot face opposite the bolt, which can exceed 20 °C for extreme cases such as Table I conditions, where the difference in spacings is large (Figure 8). Aiming to prevent these temperature variations across the mold, manufacturers often make deeper water slots adjacent to the bolts.

The calculated effect on temperature of adding deeper water slots to a mold with relatively equal slot spacing is shown in Figure 17. Calculations were performed for Table II conditions using the 3-D segment model. The section shown was taken 330 mm below the top of the mold, where heat flux was 1.6 MWm^{-2} and did not change sharply with vertical distance down the mold.

The effect of deepening the slots (from 21 to 27 mm in this 42 mm thick portion of the mold) is shown, by comparing Figures 17 a) and c). Deepening the slots lowers the hot face temperature locally by about 15°C. This tends to cool the hot face opposite the bolt.

When the depth of the bolt hole in the copper exceeds the length of bolt penetration, an air gap is created. The effect on heat transfer is of equal importance to the distance between slots. As shown in Figure 17 b), a 5 mm air gap at the bolt hole root increases the hot face temperature opposite the bolt by 10°C in a mold with equal slot depth (22.5 mm deep). Making the slots deeper beside the bolt more than compensates for this. The result is a hot face surface which still has 10 °C variations (if the slot spacing is roughly uniform).

It is interesting to note by comparing Figure 17 c) and d) that, with a deep slot beside it, the gap has relatively little effect on temperature. This remains true so long as the slot root is closer to the hot face than the air gap.

It is clear that adding deeper slots has the potential to improve temperature uniformity across the mold surface. However, deep slots also preferentially concentrate permanent residual stress at their roots. Figure 14 shows that both operating and residual stresses at the root of the deep slot are much higher than at the shallow slots. Stress at the shallow slot roots are similar to that in a mold with equal slot depth. Thus, stress concentration at the slot roots can be lowered with equal slot depths. This effect is greatest when width expansion is partially constrained, as in Figure 14. The benefit of equal slots is less significant when expansion is unconstrained.

7.2 Effect of Water Slot Root Shape

The effect of using square versus round water slot roots on effective stress during operation and residual inelastic strain is compared in Figures 18 and 19. Calculations were performed using a highly refined 2-D model for Table II conditions, with hot face heat flux increased to 3.5 MWm^{-2} (maximum temperature 352°C). The contour plots of both of these fracture criteria clearly show that stress and strain is concentrated at the slot roots, particularly the deepest slot. This location is thus prone to initiate fatigue cracks. The effect of the sharp corner of the square slot is surprisingly small. While maximum stress at the rounded slot is lower, the maximum residual strain is higher. This is because the maximum stress and strain concentrations are actually found exactly at the center of the slot root. The effect of slot root shape on both heat transfer and distortion is negligible. Thus, the benefit of using rounded slots to improve fatigue crack resistance is not clear.

(a) with square slot roots
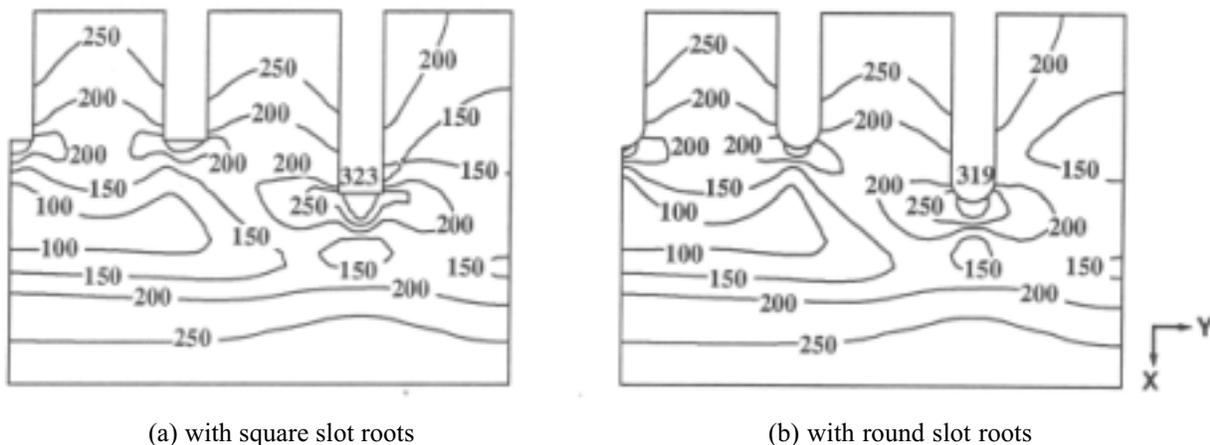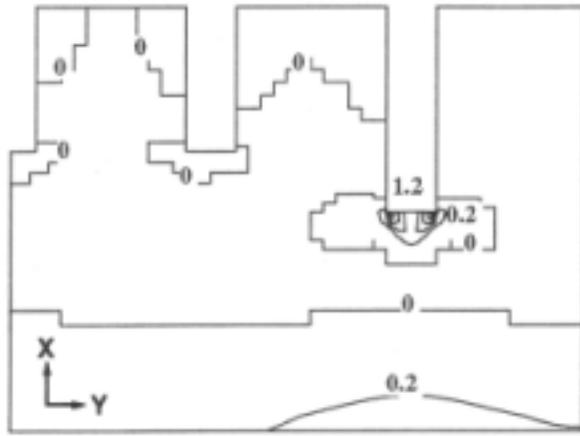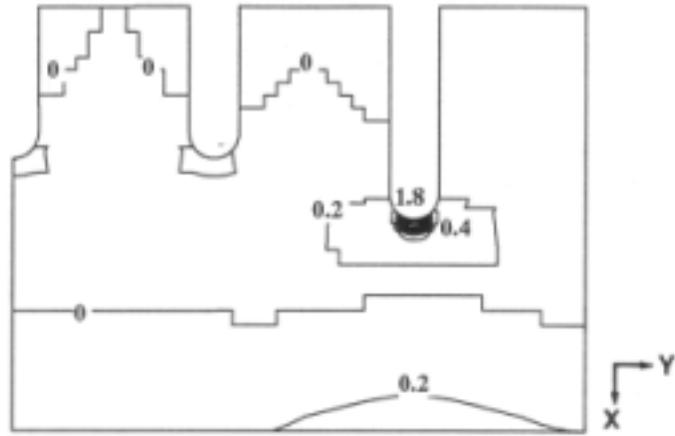(b) with round slot roots

Figure 18 Effect of round versus square slot shape on Von-Mises stress during operation (MPa) (2-D section)

(a) with square slot roots   (b) with round slot roots

Figure 19 Effect of round versus square slot shape on total residual inelastic strain (%) (2-D section)

7.3 Effect of Meniscus Level

At the top and bottom of the mold, the water slots end with curved surfaces that direct water into and out of holes in the water jacket front plate. This creates a much larger effective thickness in these extremities of the mold. Raising the meniscus level above the point where the slots first become shallower greatly increases hot face temperature. This effect was quantified with the 2-D vertical section model by translating the heat flux profile up the mold to simulate different meniscus levels in a straight-walled 55mm thick mold, with 25mm deep slots and other conditions in Table II. Figure 20 shows that the maximum hot face temperature is 336°C, when the meniscus level is 84mm or more below the top of the mold (z<816mm). Raising the level 32 mm (to z=848mm) increases this maximum temperature to 380°C. Further raising the level to the end of the water slot (z=870mm), increases the maximum temperature by over 100°C, reaching almost 450°C. In addition to aggravating creep due to the higher temperature, this detrimental practice makes the hot face temperature very sensitive to minor changes in meniscus level.
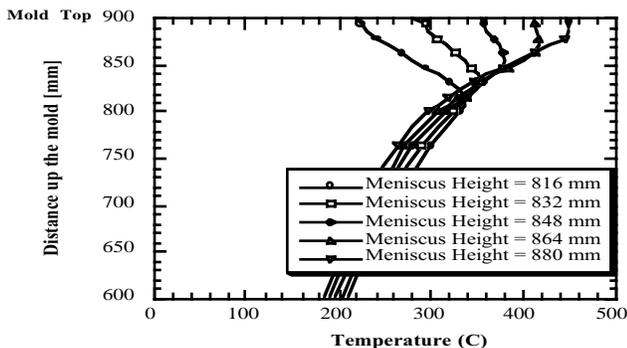

Figure 20 Effect of meniscus level on mold temperature

7.4 Effect of Heat Input

Mold distortion and stress increase directly with increasing mold temperature. Mold temperature increases directly with increasing heat input to the mold, which depends on casting speed, mold powder, oscillation mark depth, mold taper, and other factors which affect the size of the interfacial gap. To investigate the combined effect of all of these variables on mold behavior, model simulations were conducted for a "high heat flux" condition, based on data from [17]. Eq. 3 was increased by a factor of 1.4 (peak heat flux = 3.8 MWm^{-2}) and the water slot heat transfer coefficient decreased to 20 kWm^{-2}K^{-1}. Figure 21 shows that this increase in mold heat flux produces higher mold temperatures and a greater relative difference between the maximum and minimum distortions down the wide face. The greater distortion of the wide face towards the steel is balanced by the increased distortion of the narrow face, which moves the wide face away from the steel. Thus, the effect of increasing heat flux on distortion in the transverse (y-z) plane is even larger. This finding is consistent with the observations of Carlsson et. al. [19] who reported a strong correlation between increased oscillation frequency, increased total mold heat transfer and increased mold distortion. The effect of heat input on stress is even more important. The higher temperatures which accompany higher heat input increase stress during operation, creep, residual stress and residual distortion.

7.5 Effect of Copper Plate Thickness

The effect of varying thickness of the wide face copper plates was studied by simulating three different 1933 mm-wide molds, otherwise based on Table I conditions:
a) 30 mm thick copper plates with 20 mm deep slots
b) 30 mm thick copper plates with 10 mm deep slots
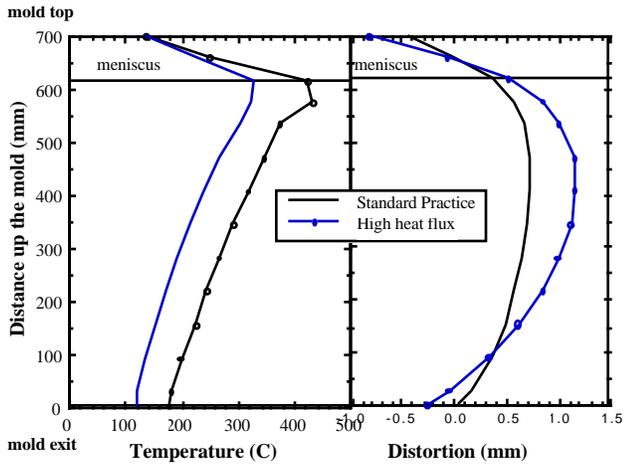c) 55 mm thick copper plates with 25 mm deep slots

Figure 21   Effect of heat flux on mold temperature and distortion (3-D quarter mold down wide-hotface centerline)

Figure 22 shows the effect on the predicted temperature and distortion, using the 3-D quarter mold model. Comparing molds a) and c) shows that decreasing the resistance to heat flow with the thinner plate lowers the hot face temperature. This produces a corresponding decrease in both distortion and thermal stress, both during
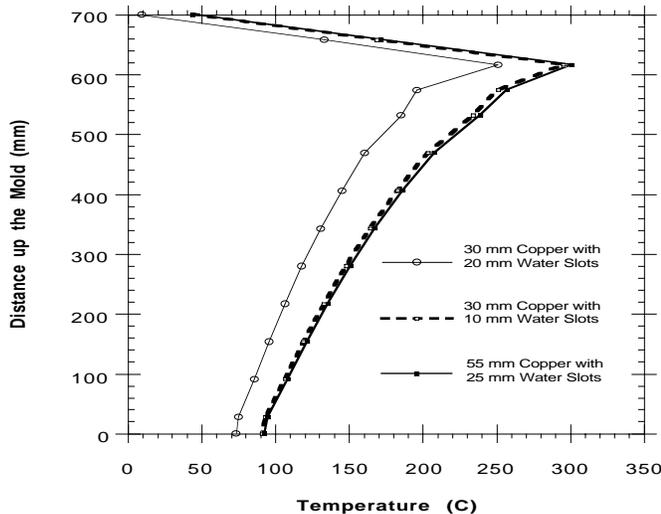
operation and after cooling to ambient. This agrees with the results of Samarasekera et al. [4] in billet molds and Hashimoto et al. [5] in slab molds.

Figure 22 mold b) shows that this logical relationship is complicated by the independent effect of the cooling water slot depth. For the same effective distance between the water slot roots and the wide hotface, deeper cooling slots act like fins to remove heat more efficiently and lower the mold temperature. Thus, the shallower cooling slots of mold b) offset its smaller effective thickness, making its temperature similar to mold c). Mold a) is much cooler than mold b) because the deeper slots both lower the effective thickness and increase the fin cooling effect. The water slots have relatively less effect on distortion and stress. Mold b) has nearly the same distortion as mold c) because its temperature is about the same. The slightly greater distortion shown for mold c) in Figure 22 is likely due to the modeling assumption of solid copper slots, although this effect is not huge. These results show that the effect of plate thickness on mold distortion is due almost entirely to its effect on hot face temperature.
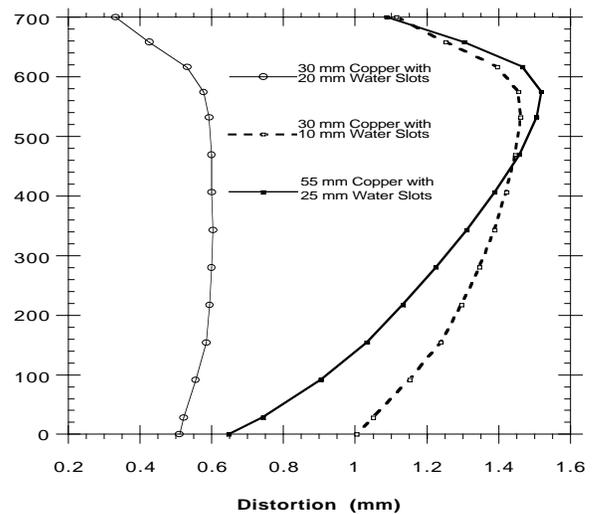

Figure 22 Effect of copper plate thickness on a) temperature and b) distortion down wide-face centerline

For the same water slot depth, thinner molds are more affected by surface temperature variations due to uneven water slots and surface shape variations due to bolt prestress. Figure 22 shows that both of the thinner, more flexible mold plates, a) and b), are forced to conform more closely to the water jacket, producing less relative distortion between the upper portion and bottom of the plates. This gives thin molds a different distorted shape than thicker molds, which have more relative distortion.

It is important to recall that the mold plates become thinner with each remachining. This lowers the temperature, distortion, and magnitude of stress imposed

on subsequent thermal cycles. However, the residual stress already present at the slot roots continues to accumulate. Older (and thinner) mold plates therefore may be more prone to catastrophic crack failure, so should be monitored more closely.

7.6 Effect of Water Jacket Rigidity

The effect of water jacket rigidity was investigated by increasing the thickness of the water jacket from 255 to 320 mm, for conditions of Ozgu [8] and Table I. At the same time, the steel plate thicknesses were increased from 30 to 40 mm. As shown in Figure

23, this increase in water jacket rigidity greatly decreases the distortion. This is also shown in Figure 15, where the experiments correspond with the more-rigid water box. Unfortunately, preventing the distortion during operation increases the stresses, so the rigid water box may be more detrimental to mold life.
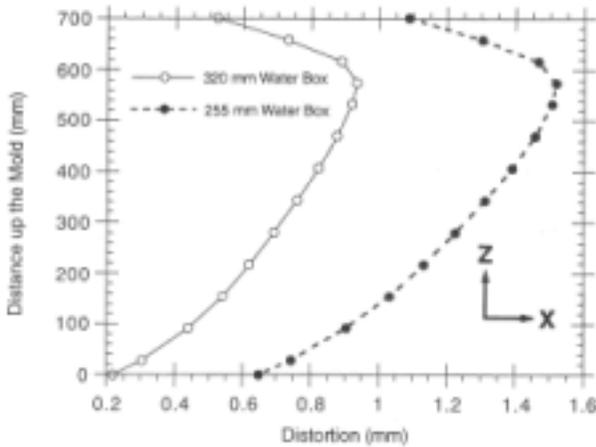

Figure 23 Effect of water jacket rigidity on distortion

7.7 Effect of Water Jacket Front Bolt Hole Size

The bolt holes in the front of the water jacket partially constrain lateral expansion of the bolts and copper plates. Figures 12 and 14 show the stress-strain histories for standard constraint conditions ("unconstrained") and for conditions of "partial constraint". The partial constraint condition simulates a 1680 mm wide plate with 19 mm bolts in oversized 23 mm diameter bolt holes. Width displacement was prevented after allowing 0.24% total y-strain in the segment model during operation, which corresponds to 2 mm of wide face expansion (each side) before the bolts contact the edge of the bolt holes. This analysis implies that the bolts closest to the mold edges are the most critical. In extreme cases of constraint by the bolt holes, the shear stress caused by thermal expansion can fracture the bolts.

Increasing constraint greatly increases inelastic strain and stress in the early thermal cycles. Figure 12 shows that the residual strain after the first cycle is -0.08% at the surface of the partially constrained plate, compared with only -0.02% for an unconstrained plate. This suggests that oversizing of the bolt holes is very beneficial, particularly near the wide face edges, where the most expansion occurs. The bolt hole size should be designed to accommodate the maximum expansion, which occurs during casting of the widest slab.

7.8 Effect of Strand Width

Moving the narrow faces to cast a wider slab produces a significant increase in mold distortion. This can be seen in Figure 24, which compares the calculated distortions of the outside of the backing plate for 914 mm and 1320 mm slabs. Wider slabs experience more distortion because the larger surface area for heat input produces more total bending strain in the wide face copper plates. The total width expansion increases in direct proportion with the slab width. The distorted shape remains about the same, with the maximum x-direction distortion always found between the meniscus and half-way down the wide face centerline.
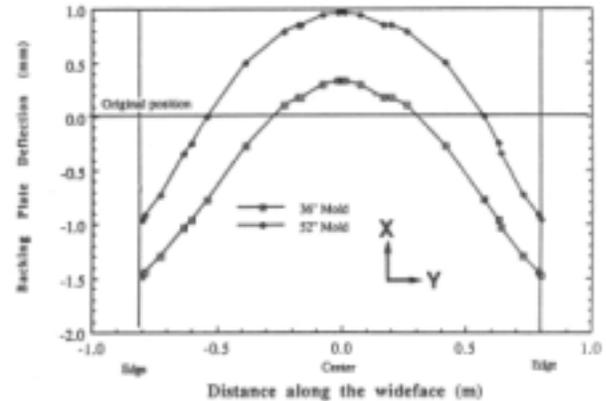

Figure 24 Effect of strand width on distortion

During a campaign, many different slab widths are cast. Stress in the copper increases with width, if there is increased constraint by the bolt holes. Maximum stress and the severity of thermal fatigue cycles are thus controlled by the maximum width cast. If the holes are oversized, then stress should remain relatively unchanged with width.

7.9 Effect of Clamping Force and Ferrostatic Pressure

The effects on distortion of removing the mold clamping forces and ferrostatic pressure are shown in Figure 25. Applying the clamping forces from Table I reduces thermal distortion, but only by about 0.1 mm. More importantly, the restraining effect of the clamping force must be transmitted across the thin line of contact between the edge of the narrow face and the wide face. Figure 26 shows that the distorted narrow face edge touches the wide face only along a short distance between the meniscus and midheight. This portion of the narrow face edge is subjected to a tremendous stress concentration, which can cause serious permanent deformation, especially just below the meniscus where high temperature enhances creep.
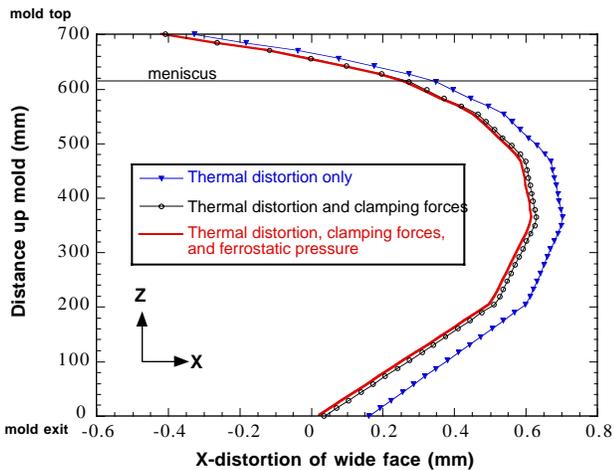
Figure 25   Effect of clamping forces and ferrostatic pressure on mold distortion

Figure 26   Distortion of wide and narrow face along the line where they meet in the mold

To minimize this problem, it is best to apply the minimum clamping forces needed to overcome the ferrostatic pressure. Thus, the total clamping force on each water jacket, F_t should increase with strand width, W, and effective mold length, L, according to:

$$F_t = 0.5 \rho g L^2 W + F_c \qquad (10)$$

where F_c is an extra force (safety factor) to keep the mold together, such as 2 kN per loading point. To avoid adverse moments which rotate the wide face against the narrow face meniscus region, the bottom clamping force should be greater than the top one, as chosen in Table I conditions. The safety factor should be reduced to a minimum during an automated width change, to minimize scraping of the copper plate surface.

Figure 25 also shows that ferrostatic pressure alone has a negligible effect on reducing mold distortion. This shows that the powerful forces of thermal expansion which cause mold distortion are difficult to restrain.

Thermal distortion causes gaps to open up along the corner between the narrow face and wide faces, both near the top and bottom of the mold, as shown in Figure 26. The gap of more than 0.2 mm just above the meniscus is probably the most serious, since mold flux could penetrate, freeze, and aggravate mold wear at this critical junction. This gap increases in size over time, as the narrow face edge becomes crushed. This problem can be minimized by avoiding drastic level fluctuations which let flux into the wider part of the gap above the meniscus. The gap at the meniscus would disappear if the clamping forces at top and bottom were equal. This is detrimental, however, as the contact region shown in Figure 26 would move upward, resulting in more severe crushing of the narrow face at the meniscus. Clamping forces should balance the ferrostatic pressure to create a net zero moment about half-way down the mold. To achieve this, the lower forces generally must be more than double the upper forces.
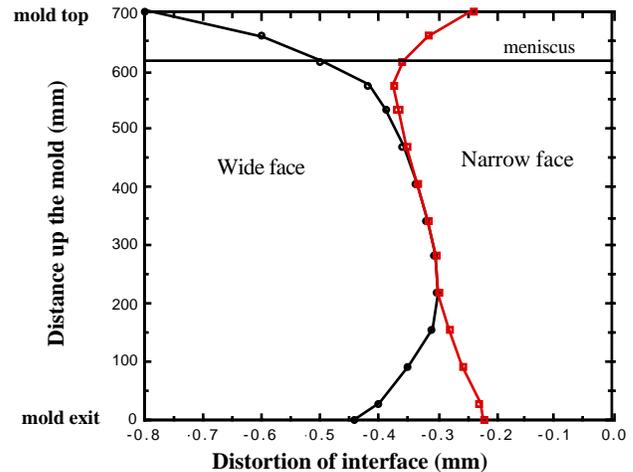
7.10 Effect of Bolt Prestress

The effect of bolt tightening was investigated by imposing a pretension of 155 MPa tension on each bolt. This corresponds to 145 N-m of torque, as shown in Appendix I. The most important effect of bolt prestress is to create tensile stress concentrations at the bolt holes on the cold side of the copper plates. This effect is greater for thicker molds.

Bolt prestress has relatively little influence on distortion (see Figure 26).   Without bolt pretension, however, the copper plates pull away from the front of the water jacket during operation (see Figures 10 and 11). With pretension, the bolts tend to pull the water jacket and copper plates together until they contact.   This prevents gap formation everywhere except at the region of maximum distortion.   The maximum reduction in thermal distortion of the copper plates is less than 0.2 mm. This is consistent with the rough calculations in Appendix I.

Friction between the copper plates and steel water jacket front is proportional to the bolt tension. This force opposes the lateral (y-z plane) movement of the plate induced by thermal expansion.   As shown in Appendix II, however, friction is negligible relative to the forces of thermal expansion, so provides little constraint. Thus, the plates are relatively free to expand, regardless of the bolt pretension.

7.11 Effect of Copper Alloy

Copper alloys are available with much higher strength and creep resistance than standard low-alloy copper. These include chromium-zirconium copper, such as CCZ and nickel-beryllium copper, such as 3HP (10). Unfortunately, the precipitates which give these alloys their higher strength, also lower their thermal conductivities, as shown in Table III. Furthermore, these conductivities decrease further with increasing temperature.

Table III. Effect of Copper Alloy

Copper alloy	Standard	CCZ	3HP
Designation	C10700	C18150	C17510
Composition (balance Cu & resid.)	0.1% Ag	.65%Cr .10%Zr	2.0% Ni 0.3% Be
Conductivity, $Wm^{-1}K^{-1}$	374	350	277
Peak temperature, ^{o}C	195	210	230
Peak distortion, mm	0.61	0.64	0.71
Peak stress, MPa (during operation)	<-305	<-335	-360
0.2% yield strength (at peak temp., MPa)	-100	-225	-535
Creep rate at peak, s^{-1}	$>10^{-8}$	$5x10^{-9}$	$2x10^{-10}$
Fraction of hot face surface above yield	~100%	18%	0%

Figure 27   Effect of copper alloy on temperature distribution in mold (wide face centerline)

To investigate the effect of copper alloy, calculations were performed during operation of a 25 mm thick mold (with 15 mm deep slots) using the 3-D quarter mold model, so temperatures and stresses are lower than for standard conditions in Table I.   As expected, higher mold temperatures are produced with higher strength (lower conductivity) copper alloys, as shown in Figure 27.   There is a corresponding increase in both mold distortion and stress levels, as given in Table III. However, the residual strains are smaller.

The results in Table III show that the weakest copper, C107, is predicted to yield in compression over almost the entire hot face surface and creep rapidly until stress levels relax. The higher strength alloys more than make up for their lower conductivities, by producing substantially lower creep rates and less plastic yielding, even when the higher temperatures and stresses are taken into account. In fact, the 3HP alloy mold is predicted to behave in a completely elastic manner.   Without permanent inelastic strain while hot, the mold should return to its original shape when it cools, with no springback, bow tie, sag, or residual stress. The resulting benefit is to reduce the need for remachining, and enable a longer mold life.
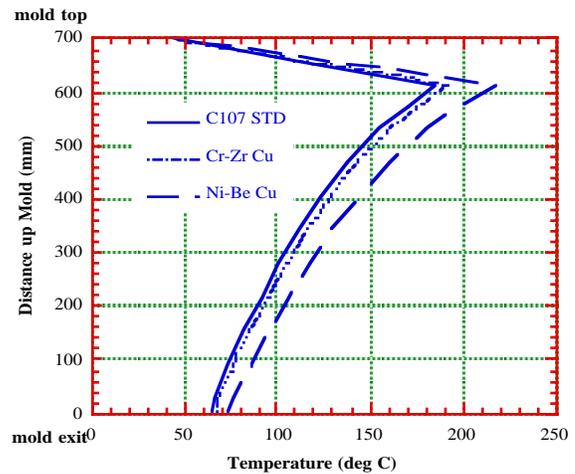
7.12 Effect on Mold Taper

Combined with shrinkage of the solidifying steel shell, the size of the gap between the shell and mold is controlled by the taper of the mold walls, which is affected by mold distortion during operation. Mold heat transfer is controlled primarily by the size of this gap, and the material filling it (mold flux or air). Even a small mold distortion significantly affects this gap.

The most important measurement is the difference between the distorted mold position at the meniscus, where the shell forms, and the distorted hot face position down the rest of the mold. Figures 11 and 21 show that down the wide face, this difference increases from zero at the meniscus to a maximum of about 0.4 mm, to roughly -0.3 mm at mold exit (Table I conditions).   This creates a negative taper of about -0.5%/m over the lower part of the mold, which greatly exceeds the 0.1%/m taper typically employed on the wide face.   Along the central portions of the wide face, ferrostatic pressure simply forces the shell to navigate around the convex mold surface.   Toward the corners, however, a negative taper exists both across and down the mold.   This likely contributes to reduced heat transfer near the corners, where the shell shrinks most and cannot readily deform to accommodate the gap.

Down the narrow face, the distorted shape of the mold during operation actually matches the natural shape of the solidifying shell more closely than would a tapered mold with no distortion. Figure 28 shows the shape of the solidifying shell, predicted with a separate solidification model [21]. The shell shrinks more near the top of the mold, where its temperature is decreasing rapidly. This figure also shows the distorted shape of the narrow face added to a simple linear taper of 1.%/m. This true shape of the tapered mold is remarkably close to the ideal shell shrinkage. This suggests that mold distortion down the narrow face is actually beneficial to steel quality.
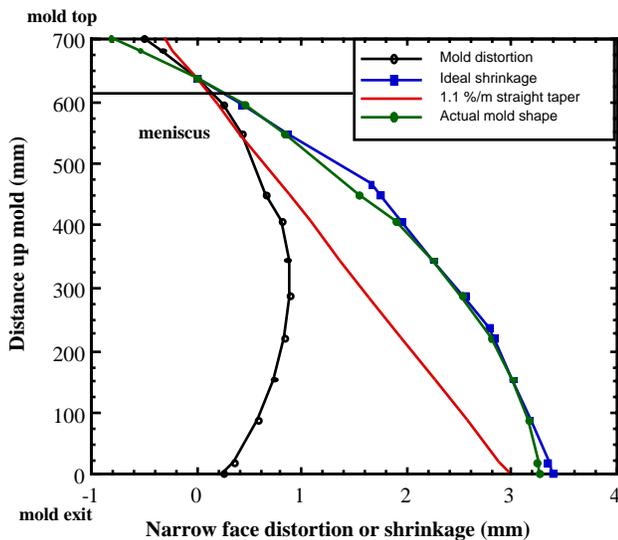
Figure 28 Comparison of predicted narrow face distortion with typical wide face shell shrinkage and mold taper pracices.

8. DISCUSSION

The results of this work have several implications for avoiding some of the important problems related to thermal and mechanical behavior of continuous slab casting molds.

8.1 Crushing Narrow Face Edge

The edge of the narrow face near the meniscus is particularly vulnerable to being crushed during operation. This is because the entire clamping force is transmitted across this very small contact area, (Figure 26) which also tends to be very hot. This leads to accelerated creep and inelastic strain, which creates a permanent gap between the narrow and wide faces at the corner. The consequences of this problem can be severe, as mold flux can enter the gap, leading to further mold wear and even a steel fin, that could initiate a sticking corner breakout in the extreme.

This problem is an unfortunate consequence of the 4-piece mold design. It can be minimized in several ways. Firstly, mold clamping forces should be reduced to the minimum necessary to balance the ferrostatic pressure. Water slots should be machined into the narrow face close enough to the corner to ensure that the critical region is adequately cooled. Finally, a high-strength, creep-resistant copper alloy is of most benefit in this region of the narrow face. The Ni-Be alloys have the best combination of properties for this purpose.

8.2 Mold Life

Mold life is reduced by the remachining needed to remove the effects of both mold wear and permanent distortion. Mold wear is usually greater in the lower portions of the wide face, due to the greater ferrostatic pressure of the steel. This can be improved by coating the copper surface with a 1-2mm layer of sacrificial nickel plating. Preferential wear on the edges of the narrow face and very near mold exit can be reduced by extending the water slots to avoid hot spots. Wear may also be high along the edges of the narrow hotface surface, particularly in the lower third the mold. This indicates excessive narrow face taper, which pushes the narrow face against resistance at its edges from the steel shell along the wide face. Scratches on mold surface accompany width changes, so clamping forces should be minimized. In addition, careful handling is needed to avoid scratches.

Permanent mold distortion contributes significantly to remachining requirements to satisfy shape specifications. It is caused primarily by high stresses, leading to plastic strain and creep. These can be minimized by lowering mold operating temperature. Unfortunately, heat flux to the hot face is difficult to control and a thinner mold reduces the available thickness for remachining. Thus, it is particularly important to avoid thermal resistances at the cold face, (such as monitoring water quality to avoid scale formation), keeping water velocity high and uniform to prevent boiling in the water slots, and by keeping the meniscus below the height up the mold where the water slots curve. Stress can also be reduced by minimizing mold constraint with oversize bolt holes and a weak water jacket. Finally, high strength copper alloys are superior in resisting both mold wear and permanent distortion.

8.3 Catastrophic Mold Cracks

Although very uncommon, it is important to consider that the most important function of the mold is to avoid cracking from the water slots to the steel. Because the strain calculated throughout the mold is always well below the ultimate fracture strain of copper, catastrophic cracks can only be initiated by thermal fatigue strain accumulation. A major fatigue cycle occurs each time the mold is filled with molten steel followed by lowering the level at least midway, such as for a nozzle tube change or end of cast. A minor cycle occurs near the meniscus during each level fluctuation.

Cracks are most likely to initiate at the roots of the deepest water slots opposite the meniscus, because this region experiences the greatest stress and strain concentration, and in the central region of the mold, which experiences a major (mold filling) cycle for every slab width. Because the hot face is in compression during operation, a crack must remain undetected and propagate very long before catastrophic sudden fracture through the remaining solid portion of the hot face can occur. This could happen during cooling, which is the only time the hot face is in tension. Because they form at lower temperatures, these cracks are likely to be primarily transgranular, except near the hot face if they connect together with a creep-related crack.

To avoid these cracks, lower mold temperature is helpful. In addition, lower mold constraint is helpful, by

using oversized bolt holes in the water jacket front, and a less rigid water box. Avoiding unequal-depth slots to minimize cracking is probably more important than the consequences of slight temperature variations across hot face temperature, which accompany equal-depth slots. The critical water slot roots should be machined carefully and inspected regularly, particularly on old molds (high number of thermal cycles) with severe bow tie, indicating high permanent creep deformation from high stress. It is naturally very important that the copper alloy have a high fatigue resistance and strain to failure. It is unknown how the fatigue crack resistance of high-strength, creep-resistant copper alloys compares with that of standard copper alloys.

8.4 Shallow Surface Cracks

Shallow, longitudinal surface cracks sometimes form on the hotface surface near the meniscus and exhibit intergranular creep fracture. They most likely initiate on the hot face opposite the deepest slots, where both stress and accumulated inelastic strain are greatest, as shown in Figs. 14b), 18, and 19. High temperature weakens the grain boundaries, so these cracks are intergranular and are more common than catastrophic cracks. Factors that minimize catastrophic cracks also help to avoid these cracks. In addition, steel level fluctuations should be avoided, because they generate the local thermal fatigue cycles of the copper hot face which create the problem. Raising the liquid level above the height where the water slots begin to curve and end is particularly detrimental.

8.5 Steel Quality Problems

Controlling mold behavior is only one of many requirements to ensure high-quality steel production. Nevertheless, mold operation can help in several ways. To help maintain uniform heat transfer in the meniscus region the meniscus level should be kept below the region where the water slots curve. This makes the mold temperature at the meniscus less sensitive to level fluctuations, which makes it easier to maintain uniform solidification conditions.

Operation with shallow surface cracks in the mold hot face at the meniscus should be avoided because they can initiate corresponding cracks in the steel shell. Coating the mold surface with nickel and / or chromium plating prevents copper pickup, which avoids star cracks. The narrow face taper should be optimized to match shrinkage of the steel shell, which requires that mold distortion to be taken into account.

Finally, the generic distortion of the mold towards the steel during operation contributes to increased interfacial gap formation along the corner and off-corner regions of the wide face. The resulting "hot spots" on the slab surface may contribute to a variety of potential quality problems, such as off-corner gutter, surface and subsurface cracks [22]. Mold distortion during operation is lower with a thicker, more rigid water jacket, and thinner, narrower, and lower-temperature copper plates. Alternatively, the wide face copper plates could be machined with a concave curvature near the corners designed to offset the thermal expansion and attain a shape during operation that matches the natural shrinkage of the shell.

9. CONCLUSIONS

Mathematical models have shed insight into thermal and mechanical behavior of the slab casting mold. The results have practical implications for minimizing potential problems, which include the following.

Detrimental residual stress and strain in the mold can be decreased by lowering mold operating temperature and minimizing constraint. This can be done in several ways including:

1) Water slots should be extended as close to the top, bottom, and edges of the mold as possible. The meniscus should not be allowed above the height where the water slot depth begins to decrease. This minimizes both mold surface temperature and temperature fluctuations.

2) Small bolt holes in the front of the steel water jacket which constrain expansion of copper plate should be avoided.

Catastrophic cracks are most likely to initiate at the root of the deepest water slot during cooling after a drop in mold level. Rounding the water slot roots does not appear to significantly reduce the danger of cracks.

Water slots should be uniform in depth in order to avoid detrimental stress concentration. The effect on copper hot face temperature variations is on the order of only 10 $^{\circ}$C.

Clamping forces should be optimized to avoid crushing the narrow face corner while balancing the ferrostatic pressure.

REFERENCES

1. Samarasekera, I. V., and Brimacombe, J. K. Ironmaking & Steelmaking **9** (1), (1982) .
2. Brimacombe, J. K., Hawbolt, E. B., and Weinberg, F. (1984) **2**, 73-84.
3. Samarasekera, I. V., and Brimacombe, J. K. (1978) *International Metals Review* **23**, 286-300.
4. Samarasekera, I. V., Anderson, D. L., and Brimacombe, J. K. (1982) *Met. Trans. B* **13B**, 91-104.
5. Hashimoto, T., et.al. (1982) *The Hitachi Zosen Technical Review* **43**.
6. Tada, K., Kasai, S., Ichihara, A., and Onishi (1987) *Kawasaki Steel Technical Report* **17**.
7. Thomas, B. G., Moitra, A., Habing, D., and Azzi, J. (1991) *in* Proceedings of the 1st European Conference on Continuous Casting , Vol. 2, pp.2 417-2.426, Associazione Italiana di Metallurgia, Florence, Italy.
8. Ozgu, M. (1995) *in* PTD Conference Proceedings, Vol. 13, Iron and Steel Society, Warrendale, PA.
9. O'Conner, T. G., and Dantzig, J. A. (1994) *Metallurgical Transactions B* **25B**, 443-457.
10. Salkiewicz, D. M., Ratka, J. O., Horn, B. D., and Natili, R. P. (1995) *in* PTD Conference Proceedings, Vol. 78, pp. 369-376, Iron and Steel Society, Warrendale, PA, Nashville, TN.
11. Savage, J., and Pritchard, W. H. (1954) *Journal of the Iron and Steel Institute* **178**, 268-277.
12. Sliecher, C. A., and Rouse, M. W. (1975) *Int. J. Heat & Mass Transfer* **18**, 677-683.
13. Zienkiewicz, O. C. (1977) The Finite Element Method, McGraw Hill, New York, NY.
14. Ratka, J. (1993), Brush Wellman Inc, Cleveland, OH, personal communication.
15. Hibbitt, Karlsson, and Sorensen (1990) , ABAQUS, Providence, Rhode Island.
16. Mahapatra, R. B., Sellers, B. T., and Young, J. D. (1988) *in* Steelmaking Conference Proceedings , Vol. 71, pp. 423-432, Iron and Steel Society, Warrendale, PA.
17. Samarasekera, I. V., and Brimacombe, J. K. (1979) *Canadian Metallurgical Quarterly* **18**, 251-266.
18. Gilles, H. L. (1990) *in* PTD Conference Proceedings, Vol. 9, pp. 123-138, Iron and Steel Society, Warrendale, PA.
19. Carlsson, G., Brolund, B., and Nystrom, R. (1989) *in* Journees Siderurgiques , ATS, Paris, Dec. 6-7.
20. Lonsbury, T. J., Fash, R. E., and Russo, T. J. (1992) *in* Steelmaking Conference Proceedings , Vol. 75, pp. 497-505, Iron and Steel Society, Warrendale, PA, Toronto, Ontario.
21. Moitra, A. (1993) , PhD Thesis, University of Illinois at Urbana-Champaign.
22. Thomas, B. G., Moitra, A., and McDavid, R. (1995) *in* PTD Conference Proceedings , Vol. 78, pp. 723-734, Iron and Steel Society, Nashville, TN.
23. Shigley, J. (1989) Mechanical Engineering Design, 5th edition, McGraw Hill, New York NY.
24. Gravemann, H. (1984) *in* Duisburger Stranggie β stage , London, UK.

APPENDIX I   BOLT PRESTRESS CALCULATION

The bolt tightening torque, τ, ranges from 65 to 110 lbs. A typical τ of 75 ft-lb (105 N-m) is related to the axial tensile force generated in the bolt by the following equation, [23]

$$F_{bolt} = \frac{2\tau}{d}\left(\frac{\pi d - \mu\lambda}{\lambda + \pi\mu d}\right) \tag{A.1}$$

where a typical 3/4-inch 10 UNC bolt has bolt diameter, d, (19 mm) and distance between threads, λ (2.54 mm). The coefficient of friction, μ, varies from 0.6 (ungreased) to 0.2 (greased), which produces bolt forces, F_{bolt}, of 16.5 kN (ungreased) to 44 kN (greased).

A force of 44 kN was assumed in each bolt for the present model. Assuming standard conditions from Table I, this force produces axial tensile stress in the bolt:

$$\sigma = \frac{F_{bolt}}{\pi\left(\frac{D^2}{4}\right)} = \frac{44 \text{ kN}}{\pi\left(\frac{.019mm^2}{4}\right)} = 155\, MPa \tag{A.2}$$

This prestress corresponds to an axial expansion of:

$$\Delta L = \frac{\sigma L}{E} = \frac{155\, MPa\ 280\, mm}{20\, GPa} = 0.21\, mm \tag{A.3}$$

This is the roughly the amount of mold distortion preventable by the bolt prestress.

APPENDIX II   FRICTION CALCULATION

The friction force that opposes lateral expansion of the copper plates across the front of the water jacket depends on the normal force, F_{bolt} from all of the bolts on the plate, N.

$$\tau = \mu\, N\, \frac{F_{bolt}}{WL} = 0.6(12 * 7)\frac{44,000\, N}{1860 mm * 900 mm} \tag{A.4}$$

The maximum friction shear stress developed, τ, is 1.32 MPa. This is negligible relative to the stresses generated by thermal expansion, which are on the order of the yield stress of 225 MPa. Thus, friction forces cannot prevent relatively free expansion of the copper plates.

APPENDIX III   EFFECT OF GRAVITY

The average shear stress generated on the copper wide face due to gravity acting on the weight of the plates (which "hang" from the bolts) is:

$\tau = \rho\, g\, t = (8940 \text{ kg m}^{-3})(9.8 \text{ ms}^{-2})(0.040 \text{ m})$

$= 3.5 \text{ kPa} = 0.004 \text{ MPa}$

Thus, the weight of the copper plates is negligible relative to the bolt prestress, friction stress, and stress due to thermal expansion and contraction.